Experimental Evaluation of Nonisothermal, First-Order Reaction Kinetics

D. J. Robbins, A. J. Almquist, D. C. Timm,* J. I. Brand, and R. E. Gilbert

Department of Chemical Engineering, University of Nebraska, Lincoln, Nebraska 68588-0126

Received December 19, 1994; Revised Manuscript Received September 21, 1995®

ABSTRACT: A procedure for the analyses of nonisothermal, batch reaction data is presented. Nonlinear regression analyses based on a least-squares objective function yield kinetic rate expression parameters from a single experiment. Data collected for the thermal decomposition of benzoyl peroxide in xylene were analyzed, illustrating differential and integral analyses. The Arrhenius frequency factor and activation energy determined were in agreement with published results obtained by isothermal experiments. In addition, the regression analyses determined the initial concentration of the reactant.

Introduction

A traditional method of determining kinetic rate constants for a given chemical reaction is to run a series of isothermal batch reaction experiments and determine Arrhenius frequency factors and activation energies from that data.[1,2] An alternate experimental strategy is to collect nonisothermal data.[3–5] Proper analysis of data from a single nonisothermal experiment can yield the order of the reaction and the initial concentration of reactants as well as the values for Arrhenius rate constants. This work presents several techniques for analyzing the results of a single batch experiment where pressure and temperature are measured as functions of time for a reaction with a gaseous product. Simple numerical methods give good results for arbitrary temperature profiles. A nonisothermal, free-radical decomposition was used to illustrate the approach.

Nonisothermal analyses of specific reaction protocols are used for differential thermal analysis (DTA) and differential scanning calorimetry (DSC).[6–10] For example, in relating reaction kinetics to heats of reaction from DSC data, Kissinger[11,12] considered an nth-order reaction:

$$\frac{d\alpha}{dt} = k^* \exp\{-E/RT\}(1-\alpha)^n \qquad (1)$$

Molar concentrations were expressed as a function of extent of reaction α and time t. R is the gas constant. The method has been adopted by the American Society for Testing and Materials, ASTM E698-79. Only data specific to conversion at the maximum reaction rate $d\alpha/dt = 0$ are used in the analysis, and variables at this point are denoted by the subject "max". When temperature is a linear function of time, $T = T_0 + \beta t$, the differentiation of eq 1 yields

$$\frac{\beta}{T_{max}^2} = \frac{k^* R}{E} n(1-\alpha_{max})^{n-1} \exp\{-E/RT_{max}\}$$

Kissinger also integrated eq 1, subject to the Coats and Redfern[13] approximation for the integral of the Arrhenius exponential, $\int_0^T exp\{-E/RT\}\, dT \doteq RT^2/E \exp\{-E/RT\}(1 - 2RT/E)$, showing that

$$n(1-\alpha_{max})^{n-1} = 1 + (n-1)\frac{2RT_{max}}{E} \doteq 1$$

When the order of the reaction is not unity, the approximate value of unity is a consequence of activation energies of 120 kJ/mol and reaction temperatures of 300–400 K. Subject to this approximation, the frequency factor k^* and the activation energy E may be evaluated from a semilogarithmic correlation of $\ln\{\beta/T_{max}^2\}$ as a function of $1/T_{max}$. The order of the reaction n may be obtained if data are correlated by the expression

$$n = \frac{\beta E}{RT_{max}^2(1-\alpha_{max})^{n-1}k^* \exp\{-E/RT_{max}\}}$$

An iterative procedure is used to solve for the order of the reaction. Experiments at different scan rates β yield data for analysis.

Segal and co-workers[3–5] discussed an iterative integral method that is also capable of determining kinetic parameters in less restricted cases. Temperature was assumed to be nearly linear in time at controlled heating rates. A supplementary term accounted for deviations. A least squares objective function was incorporated into analysis. All data observed are used.

Our research extends this work by relaxing the linear temperature profile restrictions. The method is applicable to any reaction with a gaseous product regardless of reaction stoichiometry. The nonisothermal decomposition of benzoyl peroxide in a batch reactor was studied. The experimental temperature and pressure profiles of this free-radical decomposition were used directly. Classic differential and integral analyses were performed. Since the reaction studied had literature values of activation energies around 120 kJ/mol and the temperature ranged used was 340–380 K, results were also compared to an analysis using Kissinger's method.

Reaction Analysis

Reaction Mechanism. Free-radical reactions are complex, but they can be modeled by relatively simple power law rate expressions. For benzoyl peroxide, the following mechanism has been proposed.

® Abstract published in *Advance ACS Abstracts,* November 1, 1995.

0024-9297/95/2228-8729$09.00/0

Benzoyl peroxide experiences a unimolecular decomposition:[14-16]

$$PhCOO-OOCPh \rightarrow 2PhCOO^{\bullet}$$

Benzoyloxy radicals have a tendency to lose carbon dioxide, forming phenyl radicals:[17]

$$PhCOO^{\bullet} \rightarrow CO_2 + Ph^{\bullet}$$

Initially the free radicals are in a cage of solvent molecules.[18] Before they diffuse, some termination occurs, forming diphenyl and phenyl benzoate.[19] For example

$$PhCOO^{\bullet} + Ph^{\bullet} \rightarrow PhCOOPh$$

Reactions also involve the solvent. Benzene is represented by *PhH*. Both peroxy radicals and phenyl radicals compete in transfer reactions:

$$PhCOO^{\bullet} + PhH \rightarrow PhCOOH + Ph^{\bullet}$$

After free radicals separate by diffusion, induced decomposition reactions occur.[14-16] An intramolecular radical displacement reaction[17] yields

$$Ph^{\bullet} + PhCOO-OOCPh \rightarrow PhHC_6H_4COO + PhCOO^{\bullet}$$

If, instead, the phenyl radical attacks at the carbonyl oxygen[14,15]

$$Ph^{\bullet} + PhCOO-OOCPh \rightarrow PhCOOPh + PhCOO^{\bullet}$$

Kinetic Modeling. Nozaki and Barlett[14] addressed similar decomposition reactions. The major competing reactions were condensed to

$$PhCOO-OOCPh \rightarrow 2PhCOO^{\bullet} \quad (2)$$

$$2PhCOO^{\bullet} \rightarrow CO_2 + PhCOOPh \quad (3)$$

$$PhCOO-OOCPh + PhCOO^{\bullet} \rightarrow CO_2 + PhCOOPh + PhCOO^{\bullet} \quad (4)$$

Subject to the steady-state approximation for the activated intermediate, the rate of reaction for benzoyl peroxide is the sum of two rate expressions:

$$-dP/dt = k_1P + k_iP^{3/2} = dCO_2/dt \quad (5)$$

The authors integrated this expression, developing an equation that contained the reciprocal peroxide concentration P as a function of time. Analyses of two sets of isothermal data observed at the same times, but subject to distinct initial concentrations, yielded numerical values for the unimolecular decomposition rate constant k_1 and the induced decomposition rate constant k_i, 0.118/h and 0.154 (L/mol)$^{1/2}$, respectively, for benzoyl peroxide in benzene at 80 °C. Data tabulated by Bamford and Tipper[15] indicate that a modest change in temperature will not greatly alter the ratio of unimolecular and induced reaction rates. Activation energies are of the order of 116-124 and 100-116 kJ/mol, respectively.

If Nozaki and Bartlett's data are analyzed only by the first-order rate expression, a semilogarithmic correlation of concentration a a function of time is appropriate (see Figure 1). Rate constants are dependent on the initial peroxide concentration, but each data set is satisfactorily fit. The first-order rate constants are 0.162 and 0.131/h when the initial peroxide concentration is 0.197 and 0.0206 mol/L, respectively. Other authors[15] have also used a first-order approximation. Swain et al.[16] studied the decomposition of benzoyl peroxide in dioxane in the presence of olefin monomers. For active radical scavengers, the half-lives were invariant, but for poor scavengers, the half-lives were appreciably altered. Peroxide manufacturers also report half-life data.

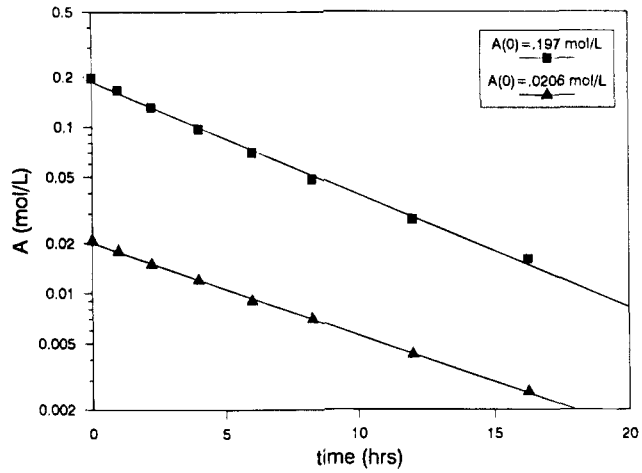

Figure 1. Analysis of Nozaki and Bartlett's data[14] by a first-order rate expression (k^* = 0.196/h when $A(0)$ = 0.197 mol/L and k^* = 0.128/h when $A(0)$ = 0.0206 mol/L).

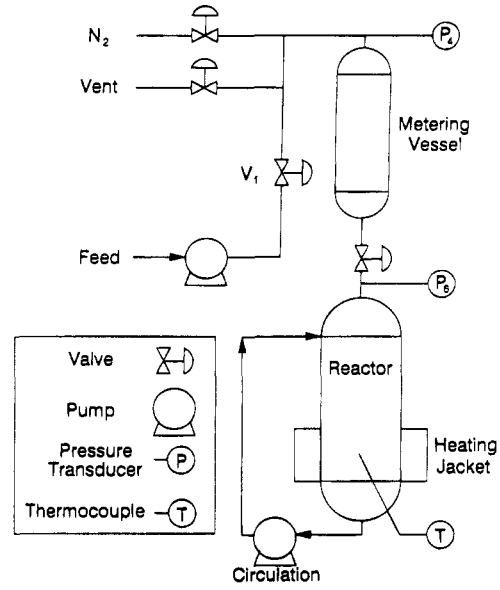

Figure 2. Sketch of experimental reactor equipment.

Experimental Procedure

A sketch of the equipment appears in Figure 2. The batch reactor was an insulated 300 mL stainless steel vessel. Electrical resistance heaters in a metal jacket around the lower third of the vessel supplied the heat. Voltage was varied using a silicon controlled rectifier in order to obtain desired temperature profiles. A J-type thermocouple measured the temperature of the liquid within the reactor. Pressure transducers with a 0-15 psig range measured the pressure in the reactor. The fluid was mixed throughout the experiment by the circulation pump. A metering vessel was located above the reactor and was at ambient temperature. The IBM personal computer was interfaced by a Keithley Metrabyte DASH-16 board.

Initially, the feed tank, metering vessel, and reactor were under nitrogen pressure. The feed tank contained benzoyl peroxide, from Atochem North American, Inc., dissolved in reagent grade xylene. The metering vessel and reactor were momentarily vented to atmospheric pressure, and the reactor was preheated to an initial temperature. The peroxide solution was pumped from the feed tank into the metering vessel. The pressure of the trapped nitrogen gas was measured by a pressure transducer P_4. When this pressure reached a set value, a numerical control algorithm shut off the feed pump and closed a pneumatically actuated valve V_1 in the feed line.

The ideal gas law was used to convert the change in pressure as measured by transducer P_4 to the volume of liquid V_{liq} within the metering vessel:

$$V_{liq} = V_{meter}\frac{P(\text{final}) - P(0)}{P(\text{final})}$$

The combined volume of the vessel and fittings is labeled V_{meter}.

After the liquid feed solution was measured, it was transferred to the reactor. The reactor was vented to atmospheric pressure and sealed. The volume of the trapped gas phase V_{gas} is the difference between the volume of the reactor and the volume of liquid.

Temperature can be controlled manually, or a numerical algorithm can produce a linear temperature ramp or an exponential temperature profile. The latter choice would allow more observations to be made at colder temperatures. The pressure in the reactor and the temperature of the liquid were recorded in equal time increments.

The selected temperature range should be based on half-life data for the reactant and the time in which the reaction is allowed to proceed. If the half-life is unknown, the operating conditions can be estimated by running the experiment from ambient temperature up to the boiling point of the solvent.

Theory

Partial Pressures. The total pressure in the reactor P consisted of the partial pressures of nitrogen, carbon dioxide, and the solvent. In an initial experiment, pure solvent was subjected to the reaction cycle. The observed xylene partial pressure was fitted with an Antoine-type relationship:

$$\ln\{p_{xyl}\} = 16.012 - 5605.8/(T + 0.2584)$$

Pressure and temperature units are psi and K, respectively. Published vapor pressure data are higher than the observed partial pressures. The vapor phase is not in equilibrium with the liquid phase for this heating protocol.

The maximum system pressure was 2 atm, absolute. Dalton's law was used to calculate the combined partial pressures for carbon dioxide and nitrogen p from the recorded pressure P:

$$p = P - p_{xyl}$$

Differential Analysis.[1,2] The molar concentration of the dissolved peroxide and the moles of gas within the closed reactor system are represented by A and G, respectively. Each mole of peroxide that decomposes is assumed to produce z moles of carbon dioxide. The rate expression was constrained to a first-order reaction:

$$\frac{dA}{dt} = \frac{-1}{zV_{liq}}\frac{dG}{dt} = -k^* \exp\{-E/RT\}A \qquad (6)$$

Integration yields

$$zV_{liq}\{A(0) - A(t)\} = G(t) - G(0)$$

For an ideal gas, the rate expression was expressed in terms of the ratio of partial pressures for carbon dioxide and nitrogen and temperature:

$$\frac{d\{p(t)/T(t)\}}{dt} = k^* \exp\{-E/RT(t)\}\left\{\frac{p(\text{large})}{T(\text{large})} - \frac{p(t)}{T(t)}\right\} \qquad (7)$$

Since eq 7 is independent of the stoichiometric ratio, z, the determined activation energy and frequency factor are independent of z as well.

After substantial reaction times at higher temperatures, the concentration of the peroxide A(large) will be zero and

$$\frac{p(\text{large})}{T(\text{large})} = \frac{p(0)}{T(0)} + \frac{zV_{liq}A(0)R}{V_{gas}} \qquad (8)$$

The partial pressure of the gas phase initially was $p(0)$ and the temperature of the fluid was $T(0)$. The nonlinear regression established the value for the constant $p(\text{large})/T(\text{large})$. The value for the initial condition $A(0)$ was then determined from eq 8, using an assigned value for z. The simplified kinetic model (discussed above) suggests a value of $z = 1$, which was used here.

The least squares objective function is

$$\Phi_1 = \sum_I \left\{k^* \exp\{-E/RT(I)\}\left\{\frac{p(\text{large})}{T(\text{large})} - \frac{p(I)}{T(I)}\right\} - \frac{d\{p(I)/T(I)\}}{dt}\right\}^2$$

The least squares error is defined by the kernel of the objective function Φ_1. Setting the derivatives of the objective function with respect to the kinetic rate parameters and a constant of integration equal to zero yields nonlinear equations which cannot be explicitly solved. The method of steepest descent[20] was used to minimize the objective function. The derivative $d\{p(I)/T(I)\}/dt$ was evaluated from a third-order polynomial, least squares fit[20] of the data set, subject to the nearest 100 observations for each point I. Savitsky and Golay[21] published tables of weights used for smoothing the equally spaced data. Corrections have been published by Madden.[22] Approximately 500 observations were used.

Integral Analysis.[1,2] The integral analysis is considered more reliable than the differential method.[24] Two integration procedures were investigated. In the first, the temperature was approximated as a linear function in time so that the Agrawal and Sivasubramanian[25] integral approximation could be used. In the second analysis, temperature data were incorporated into a numerical integration.

The integration of eq 7 yields

$$\ln\left\{\frac{p(\text{large})/T(\text{large}) - p(1)/T(1)}{p(\text{large})/T(\text{large}) - p(I)/T(I)}\right\} = k^*\int_{t_1}^{t}\exp\{-E/RT(t)\}\,dt \qquad (9)$$

An exact solution to this integral does not exist. If the temperature dependency is linear, the integral can be

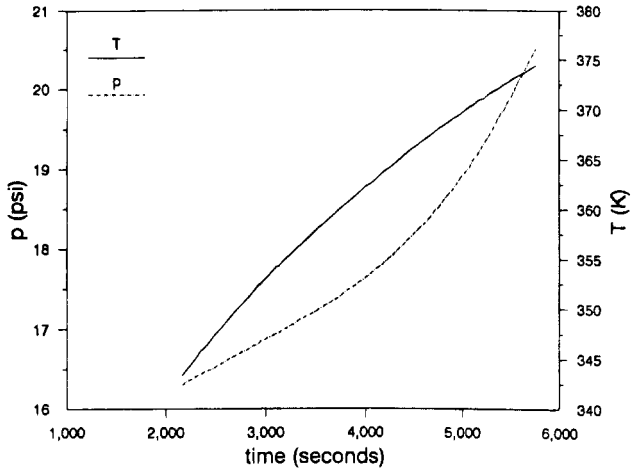

Figure 3. Partial pressure and temperature data as a function of time.

approximated by the relationship

$$\int_0^T \exp\{-E/RT\}\,dT \doteq \frac{RT^2}{E}\left\{\frac{1-2RT/E}{1-5(RT/E)^2}\right\} \times \exp\{-E/RT\} \quad (10)$$

Agrawal and Sivasubramanian[25] have shown that this approximation is superior to the Coats and Redfern[13] and the Gorbachev[26] approximations. Agrawal and Sivasubramanian reported that additional improvement can be realized if the constant 5 in eq 10 is made a function of the activation energy. However, if the value of the activation energy is not known *a priori*, then the use of the multiplication factor 5 is recommended. For arbitrary temperature histories, eq 9 must be integrated numerically. The objective function for both cases is

$$\Phi_2 = \sum_I \left\{\frac{p(\text{large})}{T(\text{large})} - \left(\frac{p(\text{large})}{T(\text{large})} - \frac{p(1)}{T(1)}\right) \times \exp(-k^* \int_{t_1}^{t} \exp(-E/RT)\,dt) - \frac{p(I)}{T(I)}\right\} \quad (11)$$

Results

The partial pressures for carbon dioxide and nitrogen plus temperature data are graphed in Figure 3 as functions of time. The temperature range was 345–375 K, and the partial pressures varied from 16.3 to 20.5 psia. The dependent variable in eq 7 is the ratio of the partial pressure to the temperature. After a least squares regression determined best estimates for the three model parameters, pressure data were simulated by integrating eq 7 to show the goodness of fit.

Differential Analysis. Data graphed in Figure 4 are a result of the differential analysis; see eq 7. Experimental temperature data were used. After the best estimates for p(large)/T(large), k^*, and E were determined, a numerical integration using the trapezoidal rule generated the p/T data from the model. The initial concentration of benzoyl peroxide $A(0)$ was estimated to be 9.41×10^{-2} mol/L when the stoichiometry coefficient z was set to one. The frequency factor and the activation energy were estimated to be 8.630×10^{13}/s and 126.1 kJ/mol, respectively. The fit has a maximum deviation from the experimental data of 0.75%. The model does tend to predict a slightly higher value for the p/T variable than the value experimentally observed. Recall that the objective function of eq 7 is

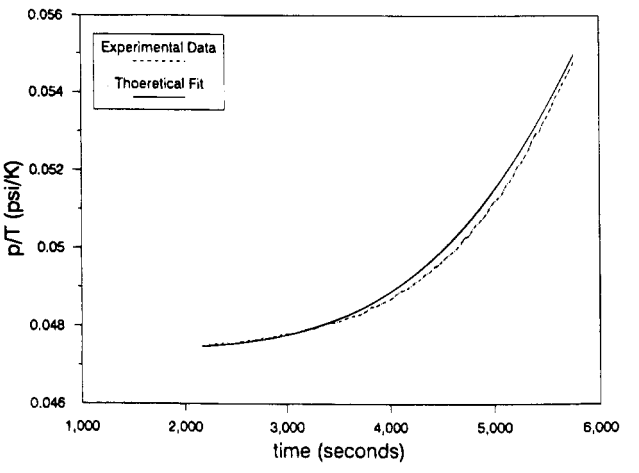

Figure 4. Results of the differential analysis, eq 7 and $A(0) = 9.41 \times 10^{-2}$ mol/L, $k^* = 8.630 \times 10^{13}$/s, and $E = 126.1$ kJ/mol.

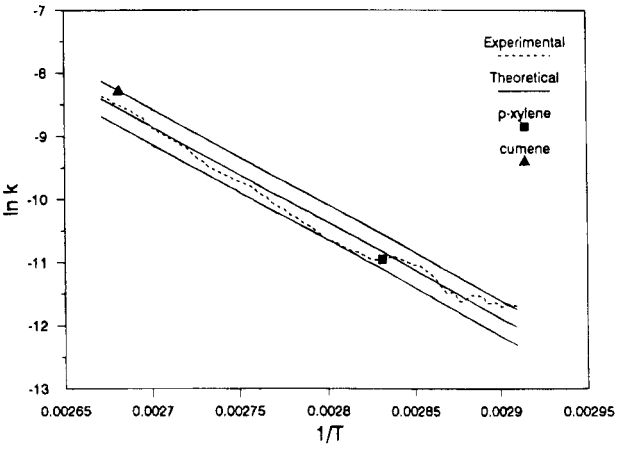

Figure 5. Correlation of ln k vs $1/T$ for the differential analysis showing the best fit line with 95% confidence intervals. Isothermal points reported by Bamford and Tipper.[15]

based on d{p/T}/dt and not on p/T. When the integration was by the Agrawal and Sivasubrananian approximation,[25] results were similar.

Data appearing in Figure 5 are consistent with an Arrhenius correlation of the rate constant as a function of temperature. The best fit line obtained from the differential analysis is shown along with the 95% confidence interval.[23] Two isothermal observations by Bamford and Tipper[15] are also shown. They are within the confidence interval.

Integral Analysis. In one integral analysis the temperature was approximated by a linear function in time so that eq 10 could be employed. Results appearing in Figure 6 illustrate the calculated and experimental data as a function of time. Maximum deviation between experimental and model values was 1.5%. The integral approximation was also used to recover pressure data from the first-order rate expression. Subject to $z = 1$, regression results were $A(0) = 8.97 \times 10^{-2}$ mol/L, $k^* = 5.603 \times 10^{13}$/s, and $E = 124.9$ kJ/mol. Figure 7 is similar except the trapezoidal rule was used to integrate the kinetic rate expression, subject to a linear temperature approximation. The same model parameters were used. This integration scheme reduced the maximum deviation to 0.91% but the fit again tends to be high.

For Figure 8 the trapezoidal rule was used for both the regression analysis and the simulation of p/T data. Actual temperature data were also incorporated into

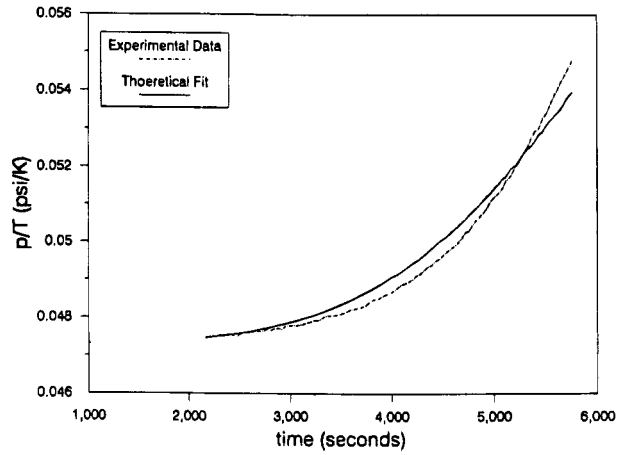

Figure 6. Results of the integral analysis, eq 10 and $A(0) = 8.98 \times 10^{-2}$ mol/L, $k^* = 5.603 \times 10^{13}$/s, and $E = 124.9$ kJ/mol. Equation 10 was used to calculate p/T from the model.

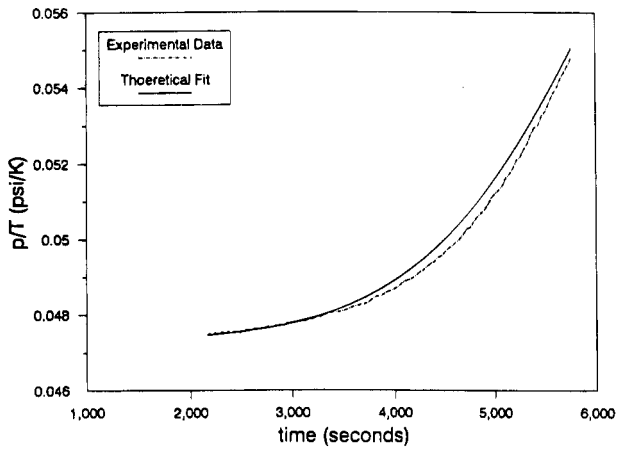

Figure 7. Results of the integral analysis, eq 10 and $A(0) = 8.98 \times 10^{-2}$ mol/L, $k^* = 5.603 \times 10^{13}$/s, and $E = 124.9$ kJ/mol. The trapezoidal rule was used to calculate p/T from the model.

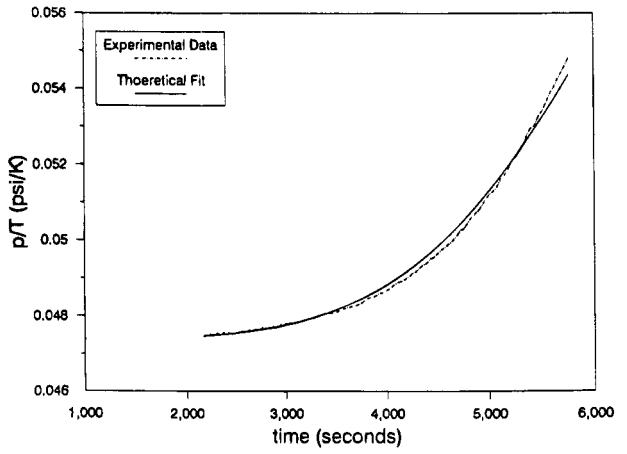

Figure 8. Results of the integral analysis, eq 9 and $A(0) = 6.38 \times 10^{-2}$ mol/L, $k^* = 6.607 \times 10^{13}$/s, and $E = 124.1$ kJ/mol. The trapezoidal rule was used to calculate p/T from the model.

this analysis. The fit between experimental data and calculated results is excellent with a maximum deviation of 0.78%. Subject to $z = 1$, $A(0) = 6.38 \times 10^{-2}$ mol/L, $k^* = 6.607 \times 10^{13}$/s, and $E = 124.1$ kJ/mol.

Discussion

A nonisothermal, batch experiment provided sufficient data to determine the Arrhenius frequency factor and activation energy and the constant of integration p(large)/T(large). Data were the easily measured physical variables, pressure and temperature, as functions of time. Ideal gas behavior was assumed. Correction was made for nonequilibrium partial pressures of the solvent. The technique does not require linear temperature profiles.

The three regression analysis schemes resulted in little scatter in the nonlinear least squares estimates of the activation energy, 124.1−126.1 kJ/mol, and in the frequency factor, $(5.603-8.630) \times 10^{13}$/s, for the thermal decomposition of benzoyl peroxide in xylene. All three analyses yielded satisfactory results. The numerical integration of actual temperature profiles yields the best results. If the temperature profiles are nonlinear, numerical integrations are recommended.

Subject to the assumption that the stoichiometric coefficient $z = 1$, the initial peroxide concentration was found to be $(6.38-9.41) \times 10^{-2}$ mol/L. The nominal initial concentration was 1.0×10^{-1} mol/L. The estimated values are reasonable. If the initial concentration of peroxide were known, the value of the stoichiometric coefficient could be calculated. Therefore, one additional experiment could provide enough information to solve for both the initial concentration and the stoichiometric coefficient.

Lenz[17] stated that $\log(k^*) = 14.2$ or $k^* = 1.58 \times 10^{14}$/s and that $E = 125.5$ kJ/mol. Bamford and Tipper[15] report frequency factors in the range of 3×10^{13} to 6×10^{14}/s and activation energies from 123.8 to 128.5 kJ/mol for benzoyl peroxide in benzene. They also report that the specific reaction rate is highly dependent on solvent effects. Data reported for decomposition rates in benzene are slightly higher than rates in solvents such as cumene and p-xylene. These specific rate constants are graphed in Figure 8 and fall within the 95% confidence interval. Nozaki and Bartlett[14] report similar unimolecular decomposition rate constants for benzoyl peroxide in a number of solvents. Our results compare favorably.

More sophisticated numerical methods might be used for both the nonlinear regression and the numerical integrations. However, for the large number of closely spaced data points here, using Simpson's rule instead of the trapezoidal rule changes the value of the integral by less than 0.002%. The method of steepest descent is not particularly efficient but is robust. Another method could be considered if computational speed is important.

Acknowledgment. Support by the Engineering Research Center and the Center for Materials Research and Analysis, University of Nebraska, Lincoln, NE, is acknowledged.

References and Notes

(1) Froment, G. F.; Bischoff, K. B. *Chemical Reactor Analysis and Design*, 2nd ed.; Wiley: New York, 1990; p 42.
(2) Levenspiel, O. *Chemical Reaction Engineering*, 2nd ed.; John Wiley & Sons: New York, 1972; p 42.
(3) Popescu, C.; Segal, E. *Thermochim. Acta* **1994**, *235*, 11.
(4) Urbanovici, E.; Segal, E. *Thermochim. Acta* **1993**, *221*, 211.
(5) Urbanovici, E.; Segal, E. *J. Therm. Anal.* **1993**, *40*, 1321.
(6) Apicella, A.; Nicloais, L.; Iannone, M.; Passerini, P. *J. Appl. Polym. Sci.* **1984**, *2083*, 29.
(7) Prime, R. B. *Polym. Eng. Sci.* **1973**, *13*, 365.
(8) Fava, R. A. *Polymer* **1968**, *9*, 137.
(9) Kamal, M. R.; Sourour, S. *Polym. Eng. Sci.* **1973**, *13*, 59.
(10) Gupta, A.; Cizmecioglu, M.; Coutler, D.; Laing, R. H.; Yavrouion, A.; Tsay, F. D.; Moacanin, J. *J. Appl. Polym. Sci.* **1983**, *28*, 1011.
(11) Kissinger, H. E. *J. Res. Natl. Bur. Stand.* **1956**, *27*, 217.

(12) Kissinger, H. E. *Anal. Chem.* **1957**, *29*, 1702.
(13) Coats, A. W.; Redfern, J. P. *Nature* **1964**, *201*, 68.
(14) Nozaki, K.; Bartlett, P. D. *J. Am. Chem. Soc.* **1946**, *68*, 1686.
(15) Bamford, C. H.; Tipper, C. F. H., Eds. *Comprehensive Kinetics*; Elsevier: Amsterdam, 1972; Vol. 5, p 492.
(16) Swain, C. G.; Stockmayer, W. H.; Clarke, J. T. *J. Am. Chem. Soc.* **1950**, *72*, 5426.
(17) Lenz, R. W. *Organic Chemistry of Synthetic High Polymers*; Wiley: New York, 1967; p 262.
(18) Franck, J.; Rabinowitch, E. *Trans. Faraday Soc.* **1934**, *30*, 120.
(19) Waits, H. P.; Hammond, G. S. *J. Am. Chem. Soc.* **1964**, *86*, 1911.
(20) Plybon, B. F. *An Introduction to Applied Numerical Analysis*; PWS-Kent: Boston, 1992; pp 187, 329.
(21) Savitsky, A.; Golay, M. J. E. *Anal. Chem.* **1964**, *36*, 1627.
(22) Madden, H. H. *Anal. Chem.* **1978**, *50*, 1383.
(23) Mandel, J. *The Statistical Analysis of Experimental Data*; Dover Publications: Mineola, NY, 1984; p 287.
(24) Flynn, J. H.; Wall, L. A. *J. Res. Natl. Bus. Stand.*, **1966**, *70A*, 487.
(25) Agrawal, R. K.; Sivasubramanian, M. S. *AIChE J.* **1987**, *33*, 1212.
(26) Gorbachev, V. M. *J. Therm. Anal.* **1975**, *8*, 349.

MA946516I